Genome-wide association studies of 27 accelerometry-derived physical activity measurements identified novel loci and genetic mechanisms

Guanghao Qi,[1]† Diptavo Dutta,[1]† Andrew Leroux,[1,2] Debashree Ray,[1,3] John Muschelli,[1] Ciprian Crainiceanu[1] and Nilanjan Chatterjee[1,4]*

[1]Department of Biostatistics, Johns Hopkins Bloomberg School of Public Health, Baltimore, MD 21205, USA

[2]Department of Biostatistics and Informatics, University of Colorado, Aurora, CO 80045, USA

[3]Department of Epidemiology, Johns Hopkins Bloomberg School of Public Health, Baltimore, MD 21205, USA

[4]Department of Oncology, Johns Hopkins School of Medicine, Baltimore, MD 21205, USA

This work was supported by an R01 grant from the National Human Genome Research Institute [1 R01 HG010480-01].

†These authors contributed equally to this work

***Correspondence to Nilanjan Chatterjee (nilanjan@jhu.edu)**

Abstract

Physical inactivity (PA) is an important risk factor for a wide range of diseases. Previous genome-wide association studies (GWAS), based on self-reported data or a small number of phenotypes derived from accelerometry, have identified a limited number of genetic loci associated with habitual PA and provided evidence for involvement of central nervous system in mediating genetic effects. In this study, we derived 27 PA phenotypes from wrist accelerometry data obtained from 88,411 UK Biobank study participants. Single-variant association analysis based on mixed-effects models and transcriptome-wide association studies (TWAS) together identified 5 novel loci that were not detected by previous studies of PA, sleep duration and self-reported chronotype. For both novel and previously known loci, we discovered associations with novel phenotypes including active-to-sedentary transition probability, light-intensity PA, activity during different times of the day and proxy phenotypes to sleep and circadian patterns. Follow-up studies including TWAS, colocalization, tissue-specific heritability enrichment, gene-set enrichment and genetic correlation analyses indicated the role of the blood and immune system in modulating the genetic effects and a secondary role of the digestive and endocrine systems. Our findings provided important insights into the genetic architecture of PA and its underlying mechanisms.

Key words: Genome-wide association studies, physical activity, novel loci, blood and immune mechanisms

Introduction

Regular physical activity (PA) is associated with lower risk of a wide range of diseases, including cancer, diabetes, cardiovascular disease(Kyu et al., 2016), Alzheimer's disease(Rovio et al., 2005), as well as mortality(Smirnova et al., 2019; Leroux et al., 2019). However, studies have indicated that large majority of US adults and adolescents are insufficiently active(Piercy et al., 2018), and thus PA interventions have great potential to improve public health. PA was shown to have a substantial genetic component, and understanding its genetic mechanism can inform the design of individualized interventions(Lightfoot et al., 2018; Moore-Harrison & Lightfoot, 2010). For example, people who are genetically pre-disposed to low PA may benefit more from early and more frequent guidance.

A number of previous genome-wide association studies (GWAS) on physical activity have relied on self-reported phenotypes, which are subject to perception and recall error(De Moor et al., 2009; Hara et al., 2018; Kim et al., 2014; Klimentidis et al., 2018). Recently, wearable devices have been used extensively to collect physical activity data objectively and continuously for multiple days. To date, there have been two GWAS based on acceleromtery-derived activity phenotypes. Both studies used data from the UK Biobank study(Doherty et al., 2017; Bycroft et al., 2018) but only focused on a few summaries of these high-density PA measurements. One study considered two accelerometry-derived phenotypes (average acceleration and fraction accelerations > 425 milli-gravities) and identified 3 loci associated with PA(Klimentidis et al., 2018). A second study used a machine learning approach to extract PA phenotypes, including

overall activity, sleep duration, sedentary time, walking and moderate intensity activity(Doherty et al., 2018). This study identified 14 loci associated with PA and found that the central nervous system (CNS) plays an essential role in modulating the genetic effects on PA. However, both studies used a small number of phenotypes, which may not capture the complexity of PA patterns.

Recent studies suggest that in addition to the total volume of activity, other PA summaries may be strongly associated with human health and mortality risk. For example, the transition between active and sedentary states was strongly associated with measures of health and mortality(Leroux et al., 2019; Schrack et al., 2019). PA relative amplitude, a proxy for sleep quality and circadian rhythm, was strongly associated with mental health(Rock, Goodwin, Harmer, & Wulff, 2014a). Moderate-to-vigorous PA (MVPA) and light intensity PA (LIPA) have also been reported to be associated with health(McGregor, Palarea-Albaladejo, Dall, Stamatakis, & Chastin, 2019; Young & Haskell, 2018). Thus, there is increasing evidence that objectively measured PA in the free-living environment is a highly complex phenotype that requires a large number of summaries that provide complementary information. Understanding the genetic mechanisms behind these summaries is critical for understanding the genetic regulation of activity behavior and informing targeted interventions.

In this paper, we conducted genome-wide association analysis using 27 accelerometry-derived PA measurements from UK Biobank data(Bycroft et al., 2018; Doherty et al., 2017). The phenotypes cover a wide range of features including volumes of activity, activity during

88 different times of the day, active to sedentary transition probabilities, principal components
89 and proxies for circadian rhythm (**Table 1**). We conducted GWAS using a mixed-model-based
90 method, fastGWA(Jiang et al., 2019), to identify variants associated with the above phenotypes.
91 We also conducted transcriptome-wide association studies (TWAS)(Gusev et al., 2016) across
92 48 tissues to identify genes and tissues harboring the associations. We further conducted
93 colocalization (Giambartolomei et al., 2014), tissue-specific heritability enrichment(Finucane et
94 al., 2018; Finucane et al., 2015), gene-set enrichment(Watanabe, Taskesen, van Bochoven, &
95 Posthuma, 2017) and genetic correlation(Bulik-Sullivan et al., 2015a) analyses to further reveal
96 the underlying biological mechanisms. We identified 5 novel loci associated with PA and
97 showed that, in addition to the CNS, blood and immune related mechanisms could play an
98 important role in modulating the genetic effects on activity, and digestive and endocrine tissues
99 could play a secondary role.
100
101 **Material and Methods**
102
103 *Study Cohort and Physical Activity Phenotypes*
104
105 The UK Biobank study consists of ~500,000 individuals in the United Kingdom with
106 comprehensive genotype and phenotype data(Bycroft et al., 2018). We used a subset of the
107 103,712 individuals who were invited and agreed to participate in the accelerometry sub-study
108 where participants wore a wrist-worn accelerometer for up to 7 days(Doherty et al., 2017).
109 Accelerometry data from participants are available at multiple resolutions. Here, the individual-

specific set of accelerometry-based phenotypes was derived from the five-second level acceleration data provided by the UK Biobank team. We further compressed the data by averaging the 5-second level data within every minute. Individuals were screened for poor quality data using indictors provided by the UK Biobank. In addition, we required individuals to have at least 3 days (12am-12am) of sufficient wear time defined as estimated wear time greater than 95% of the day (>= 1368 minutes). Our inclusion criteria for this analysis closely mirrors that described in a related paper from our group(Leroux et al., 2020) with the exception that we did not exclude participants younger than 50 at the time of accelerometer wear or based on missing demographic and lifestyle data and instead excluded individuals based on ancestry and genotype data (see subsection *Genotype Data* below).

Physical activity phenotypes were all calculated at the day level and then averaged within study participants across days to obtain one measure for each phenotype and study participant. This led to in 31 PA phenotypes for 93,745 study participants that covered a wide spectrum of information. The phenotypes are described in **Table 1** and briefly summarizes as follows: 1) total volume of activity (total acceleration (TA), total log acceleration (TLA)); 2) activity during 12 disjoint two-hour windows of the day (TLA 12am-2am, TLA 2am-4am, …, TLA 10pm-12am); 3) duration of sedentary state (ST), LIPA and MVPA; 4) principal components of the log-transformed minute-level activity profiles (PC1-6); 5) active-to-sedentary transition probability (ASTP) and sedentary-to-active transition probability (SATP); 6) proxy phenotypes for circadian patterns, including dynamic activity ratio estimate (DARE), activity during the most active 10 hours (M10) and least active 5 hours (L5) of the day, timing of M10 and L5, and PA relative

132 amplitude ($\frac{M10-L5}{M10+L5}$). They included most of the phenotypes used in the previous PA association

133 studies as well (See **Table 1** for details)(Doherty et al., 2018; Klimentidis et al., 2018). The exact

134 procedure for deriving study participant-specific phenotypes is described in detail in the

135 supplemental material of the related paper from our group(Leroux et al., 2020). The

136 phenotypes were inverse-normal transformed

137 $$INT(y_i) = \Phi^{-1}\left[\frac{rank(y_i)-k}{n-2k+1}\right], \quad k = 3/8,$$

138 where the transformed variables have mean 0 and variance 1.

139

140 *Removing Highly Correlated Phenotypes*

141

142 Some of the initial 31 PA phenotypes were highly correlated (**Figure S1**). To avoid counting

143 similar phenotypes multiple times, if two phenotypes had correlation > 0.8 we removed one of

144 them. First, we removed total acceleration (TA), duration of sedentary state (ST), PC1 and M10

145 due to their high correlation with total log acceleration (TLA). TLA was retained as the main

146 metric for the total volume of activity. Since two previous GWASs used TA as the main metric

147 for the volume of activity (Doherty et al., 2018; Klimentidis et al., 2018), we chose TLA instead

148 of TA to avoid repetition with existing work. In addition, the original distribution of TA is highly

149 skewed, which may not be completely addressed by the INT. In total, 4 phenotypes were

150 removed and 27 PA phenotypes were retained for the association analysis.

151

152 *Genotype Data*

153

154 The imputed genotype data for ~93 million variants, using UK10K, 1000 Genomes (Phase 3) and
155 Haplotype Reference Consortium as reference panel, provided by UK Biobank were used and
156 merged with the PA phenotype data. Following the Neale lab UK Biobank GWAS pipeline
157 (https://github.com/Nealelab/UK_Biobank_GWAS/blob/master/imputed-v2-
158 gwas/README.md), we excluded study participants according to the following criteria: 1) non-
159 white ancestry; 2) putative sex chromosome aneuploidy; 3) an excessive number of relatives
160 (more than 10 putative third-degree relatives in the kinship table); 4) sample was not in the
161 input for phasing of chr1-chr22. After applying these exclusion criteria the sample was further
162 reduced to 88,411 study particiants for downstream analysis.
163
164 We conducted variant quality control to ensure that genetic variants with poor genotyping
165 quality do not affect the results. Specifically, variants that satisfy any of the following criteria
166 were removed: 1) imputation INFO score < 0.8; 2) MAF < 0.01; 3) Hardy-Weinberg Equilibrium
167 (HWE) p-value < 1×10^{-6}; 4) missing in more than 10% study participants. After the filtering,
168 8,951,705 variants remained for downstream analysis, of which 8,067,228 (90.1%) were single
169 nucleiotide polymorphisms (SNPs) and the rest (9.9%) were insertion-deletions (INDELs).
170
171 *Association Analysis*
172
173 We used a fast mixed-effects model method, fastGWA(Jiang et al., 2019), for genome-wide
174 association analysis. Like other mixed-effects model methods, fastGWA allows the inclusion of
175 related and unrelated individuals but improves computational efficiency by incorporating a

176 sparse genetic relationship matrix (GRM). The GRM measures the genetic similarity between
177 individuals and each element is the correlation of genotypes between a pair of individuals. We
178 constructed the GRM using linkage disequilibrium (LD)-pruned variants that had MAF > 5% and
179 were present in HapMap3 (LD-pruning was done in PLINK using the following set up as
180 recommended in Jiang et al (Jiang et al., 2019): window size = 1000Kb, step-size = 100 and r^2 =
181 0.9). We further computed a sparse-GRM at sparsity level 0.05 to capture the genetic
182 relatedness between the closely related individuals only and reduced others to zero. We used
183 the Haseman-Elston regression to estimate the variance of the random effects as an
184 intermediate step of fastGWA. This approach is orders of magnitude faster than the previous
185 state-of-the-art, BOLT-LMM(Loh et al., 2015; Loh, Kichaev, Gazal, Schoech, & Price, 2018).
186
187 Models were adjusted for age, sex and the first 20 genetic principal components as covariates.
188 Because the PA phenotypes are correlated, principal component analysis (PCA) was conducted
189 on the phenotypes to estimate the number of independent phenotypes before setting the
190 GWAS significance threshold. At least 19 phenotype PCs were needed to explain 99% percent of
191 the PA phenotypic variance (**Figure S2**). Variants with p-value below the threshold
192 $5 \times 10^{-8}/19 = 2.63 \times 10^{-9}$ were declared to be statistically significant, which accounted for
193 the number of independent phenotypes. LD clumping was conducted based on the minimum p-
194 value across phenotypes. The requirements for the lead SNPs of different loci were to have
195 $r^2 < 0.1$ and be at least > 500kb apart.
196

197 A locus was defined as novel if its lead variant is >500kb from the lead variant of any known loci
198 discovered by the following GWASs on PA, sleep, and circadian rhythm: (1) Doherty et al study
199 on a smaller set of accelerometry-derived PA phenotypes(Doherty et al., 2018); (2) Klimentidis
200 et al study on self-reported and accelerometry-derived PA(Klimentidis et al., 2018); (3) Dashti et
201 al study on self-reported sleep duration(Dashti et al., 2019); (4) Jones et al study on circadian
202 rhythm(Jones et al., 2019). Considering the diversity of PA phenotypes, we further ensure these
203 loci do not have associations with other related traits not listed above, by searching for the lead
204 variants in Open Targets Genetics (OTG, https://genetics.opentargets.org/). A locus remains
205 novel if the lead variant: 1) is not associated at $p < 5 \times 10^{-8}$ with traits whose names include
206 the following keywords: accelerometry, physical, exercise, sleep, nap, circadian and
207 chronotype; 2) and is not in LD with previously reported GWAS lead variants for these traits
208 ($r^2 > 0.5$).
209
210 Transcriptome-wide association studies (TWAS) were conducted using the FUSION R
211 program(Gusev et al., 2016) with reference models generated from 48 tissues of GTEx v7(GTEx
212 et al., 2017). TWAS analysis was limited to the 18 traits with at least one genome-wide
213 significant variant ($p < 2.63 \times 10^{-9}$). Multiple testing due to the large number of tissue-trait
214 combinations (48*18=864) was addressed by a two-stage adjustment approach: 1) for each
215 variant, the Benjamini-Hochberg (BH) adjustment was applied across all tissue-trait pairs; 2)
216 each variant with BH-adjusted p-value 2.5×10^{-6} was then identified (accounting for 20,000
217 protein-coding genes). Since there can be multiple genes in close proximity to each other, to
218 identify independent loci detected by TWAS analysis, genes were clustered based on significant

219 associations. A clumping approach was used, which selected the gene with the smallest
220 minimum p-value across tissue-trait pairs and removed the other genes with a transcription
221 start site (TSS) within 1Mb of the lead gene TSS. The process continued by identifying the gene
222 with the next smallest minimum p-value and iterating. The only exception was when the lead
223 gene of the cluster was not a protein-coding gene (e.g., pseudogene, lncRNA) and a protein-
224 coding gene was in the cluster. In this case the protein-coding gene with the smallest minimum
225 p-value was identified as the lead gene. This led to independent gene clusters at genomic loci
226 which were least 1Mb apart, i.e., none of the lead gene TSS is within the cis region of another
227 lead gene.
228
229 *Enrichment Analysis*
230
231 Stratified LD score regression(Finucane et al., 2015; Finucane et al., 2018) was used to identify
232 the tissues and genomic annotations enriched by the heritability for PA. For tissue specific
233 analysis, chromatin-based annotations were used as derived from the ENCODE and Roadmap
234 data(ENCODE, 2012; Roadmap et al., 2015) by Finucane et al(Finucane et al., 2018). The
235 annotations were based on narrow peaks of DNase I hypersensitivity site (DHS) and five
236 activating histone marks (H3K27ac, H3K4me3, H3K4me1, H3K9ac and H3K36me3) observed for
237 111 tissues or cell types, resulting in a total of 489 annotations. Stratified LD score regression
238 computes the heritability attributed to each annotation and computes a coefficient and a p-
239 value that characterize enrichment.
240

241 In a separate analysis, the enrichment of TWAS signals was evaluated among the genes that
242 have been reported to be associated to different traits, using FUMA(Watanabe et al., 2017;
243 Watanabe, Umićević Mirkov, de Leeuw, van den Heuvel, & Posthuma, 2019). For a given PA
244 trait, we defined a gene-set as the genes that were significant at an exome-wide level ($p <$
245 2.5×10^{-6}) and investigated whether these genes overlapped with the genes that have been
246 mapped to genome-wide significant variants for different traits as reported in GWAS
247 catalog(Buniello et al., 2019). The collection of such genes have been detailed in Molecular
248 Signatures Database (MSigDB)(Liberzon et al., 2011). We used FUMA to compute the
249 proportion of genes related to other diseases and traits that were also identified by our TWAS
250 analysis and computed enrichment p-values using the Fisher's exact test.
251
252 *Colocalization Analysis*
253
254 For each susceptibility locus of PA (**Table 2**), colocalization analysis was conducted between its
255 most significantly associated phenotype and eQTL effects on gene expression in 48 tissues in
256 GTEx v7(GTEx et al., 2017). SNPs within +-200kb radius of the lead SNP were used and genes
257 that had at least one significant eQTL (q-value < 0.05) in the region were considered. Analysis
258 was conducted using the R package COLOC (Giambartolomei et al., 2014) and GWAS and eQTL
259 effects were identified as being colocalized if PP4 > 0.8.
260
261 *Heritability and Genetic Correlation Analysis*
262

263 Heritability of activity phenotypes was estimated using Haseman-Elston regression as an
264 intermediate output of fastGWA(Jiang et al., 2019). Our fastGWA analysis computed sparse
265 GRM at sparsity level 0.05 as recommended by the fastGWA paper (see "Association analysis").
266 However, this cutoff may miss the subtle relatedness in the sample and affect heritability
267 estimate. As a sensitivity analysis, we re-estimated the heritability using a lower sparsity
268 threshold at 0.02 to capture more subtle relatedness. The genetic correlation between 18 PA
269 traits and 238 complex traits and diseases was estimated using LD score regression(Bulik-
270 Sullivan et al., 2015a) implemented in LD Hub(Zheng et al., 2017). In particular, we focused on
271 four broad groups of traits and diseases (A) cholesterol levels (B) anthropometric traits (C)
272 autoimmune disease and (D) miscellaneous traits including psychiatric, neurological, cognitive
273 and personality traits. For each trait and within each category, we applied a false discovery rate
274 correction to the p-values corresponding to the genetic correlation estimated using LD score
275 regression, to account for multiple testing. Any genetic correlation with FDR-adjusted p-value
276 less that 10% were declared as significant.
277
278 **Results**
279
280 *Genetic Loci Associated with Physical Activity*
281
282 Single-variant genome-wide association analysis identified a total of 16 independent loci,
283 including three novel ones compared to previous studies (**Table 2 and Figure 1**). All three novel
284 loci were discovered on chromosome 3: the locus indexed by rs3836464 was associated with

285 ASTP; the locus indexed by rs9818758 was associated with relative amplitude, which is a proxy
286 sleep behavior and circadian rhythm(Rock, Goodwin, Harmer, & Wulff, 2014b); the locus
287 indexed by indel 3:131647162_TA_T (no rsid available) was associated with TLA 2am-4am
288 which is a proxy phenotype for activity during sleep. LIPA appeared to be associated with other
289 SNPs near 3:131647162_TA_T but not the lead variant itself, indicating multiple independent
290 signals at the same locus (**Figure 1**). Nearest coding genes for the novel loci include *SEC13*,
291 *USP4*, and *CPNE4*.
292
293 Our analysis also identified novel phenotypes for several known loci (**Table 2**). The strongest
294 signal was seen for the locus indexed by rs113851554 which is associated with multiple sleep
295 and circadian rhythm proxy phenotypes including TLA 12am-2am ($p = 6.7 \times 10^{-37}$), TLA 2am-
296 4am ($p = 7.9 \times 10^{-39}$), average log acceleration during the least active 5 hours of the day (L5,
297 $p = 1.3 \times 10^{-33}$), timing of L5 ($p = 5.4 \times 10^{-22}$) and PA relative amplitude ($p = 6.9 \times 10^{-15}$).
298 This locus was previously identified to be associated with accelerometry-derived sleep duration
299 in UK Biobank(Doherty et al., 2018). Among other known loci, 5 were only discovered in the
300 GWAS of self-reported circadian rhythm(Jones et al., 2019) but not in the other studies
301 considered (**Table 2**, last column). In our analysis, the loci indexed by rs1144566, rs9369062 and
302 rs12927162 were associated with sleep proxy phenotypes including timing of L5, TLA 12am-
303 2am, TLA 2am-4am and TLA 10pm-12am. Three other loci, indexed by rs301799, rs2909950 and
304 rs12717867, were associated with TLA 6pm-8pm and LIPA, respectively.
305

306 In addition to the phenotypic associations above, other variants in some of the loci captured
307 associations that are not reflected by the lead variants. In particular, variants in high LD with
308 rs2138543 are associated with a wide range of phenotypes including LIPA, MVPA, activity
309 during two-hour windows, and a number of proxy phenotypes for circadian patterns (**Table S1**).
310
311 *Transcriptome-Wide Association Study and Colocalization Analysis*
312
313 We performed transcriptome-wide association studies (TWAS) (Gamazon et al., 2015; Gusev et
314 al., 2016) for each PA trait based on gene expression data across 48 tissues available through
315 GTEx (version 7)(GTEx et al., 2017). Our analysis identified 15 loci (**Table 3, Figure 2, Table S2**)
316 with significant association in at least one trait-tissue pair analysis after correcting for multiple
317 testing (Benjamini-Hochberg corrected p-value < 2.5×10^{-6}, see **Methods**). We identified two
318 novel loci. One of them was indexed by *RN7SKP16*, whose higher expression in brain putamen
319 basal ganglia is genetically associated with lower level of MVPA. Another was indexed by
320 pseudogene *PDXDC2P (16q22.1)*, whose higher expression in esophagus mucosa and EBV
321 transformed lymphocytes appeared to be genetically associated with lower level of TLA 6am-
322 8am (**Figure 2**). See **Table S2** for details of these associations. These loci was not previously
323 reported by any prior GWAS and were not close to any of the 3 novel regions detected by our
324 single variants analysis (**Table 3**).
325
326 The TWAS analysis also identified novel PA phenotypes, potential target genes and underlying
327 tissues for many of the known loci or novel loci detected through single variant analysis (**Table**

328 **3**). Consistent with a previous study (Doherty et al., 2018), the TWAS analysis showed that
329 genetic association for PA traits often points towards involvement of CNS (**Table 3**). Further, our
330 analysis indicates consistent involvement of blood and immune, digestive and endocrine
331 systems in modulating the genetic effects on PA. See **Table S2** for a complete list of associated
332 tissues. Among the 15 loci significant in TWAS analysis, the lead genes of 4 loci were
333 significantly associated with PA phenotypes via the blood and immune tissues. For example, the
334 genetically predicted expression of *PBX3* and *KANSL1* in the blood and immune tissues (whole
335 blood, EBV-transformed lymphocytes) were each associated with 3 PA phenotypes. The genes
336 associated with PA via blood and immune tissues were also associated via digestive (esophagus
337 mucosa, small intestine - terminal ileum, colon – sigmoid, etc) and/or endocrine (thyroid,
338 pituitary) tissues, but only one of them overlapped with the 9 genes that were associated with
339 PA phenotypes through the CNS (**Table 3**). Another locus, represented by *C3orf62*, were
340 associated with PA relative amplitude only via the digestive and endocrine tissues (esophagus
341 mucosa, colon – sigmoid, thyroid) but not the blood/immune tissues or CNS. These findings
342 suggested two potential pathways for the genetic regulation of PA: a primary pathway involving
343 the CNS (brain in particular) and a secondary pathway involving the blood/immune system and,
344 potentially, the digestive and endocrine systems. The actual biological processes involved in the
345 pathways are beyond the scope of this paper and may be worth future investigation.
346
347 Several genes that were found to be significantly associated to specific PA traits in our TWAS
348 analysis, were also found to be highly overlapping with genes that were previously reported to
349 be associated with various traits and diseases including but not limited to neuropsychiatric

350 diseases, behavioral traits, anthropometric traits and autoimmune diseases (**Figure S3**). For
351 example, we found that the genes associated with TLA across different tissues, are enriched for
352 genes that have been associated with neuroticism, bipolar disorder, Parkinson's disease,
353 cognitive function and several others indicating the putative involvement of the CNS in the
354 genetic mechanism of TLA. Additionally, the genes associated with relative amplitude
355 overlapped highly with those associated with several autoimmune diseases like inflammatory
356 bowel disease, ulcerative colitis in addition to different behavioral and cognitive traits (**Figure**
357 **S3**). These results further supported the possible involvement of both CNS as well as the blood
358 and immune system in the genetic mechanism of PA traits.
359
360 We performed a colocalization analysis to gain further insights on the tissue specific activity of
361 the significant genetic loci. Among the 16 loci significantly associated with PA, 9 loci colocalized
362 with the eQTL signals for at least one gene and one tissue with a colocalization probability
363 (PP4) > 0.8 (**Table S3**). Colocalization occurred in a similar set of tissues as those that harbored
364 the TWAS associations (**Table 3 and Table S3**), namely the CNS, blood and immune (whole
365 blood, spleen, EBV transformed lymphocytes), digestive (esophagus, colon) and endocrine
366 (thyroid, testis, adrenal gland) tissues, and also in a number of cardiovascular tissues that were
367 not highlighted by TWAS. Among the 15 lead genes for TWAS significant loci, the eQTL signal of
368 4 genes (*RERE, C3orf62, PBX3* and *RP11-396F22.1*) colocalized with PA GWAS signal in at least
369 one tissue. Colocalization also occurred in two other secondary genes (*RP5-1115A15.1* and
370 *CASC10*).
371

372 *Analysis of Heritability and Co-Heritability*

373

374 Our fastGWA analysis estimated genome-wide heritability of PA phenotypes as an intermediate
375 output. The estimates appeared to be dependent on the sparsity level of the genetic
376 relationship matrix (**Figure S4**). We chose the results under the lower cutoff (0.02) since it
377 captured more subtle relatedness and should give more accurate heritability estimates. The
378 estimates of heritability varied across different PA phenotypes. A number of traits were
379 estimated to have higher heritability than others, including TLA (0.15), TLA 6pm-8pm (0.15),
380 MVPA (0.14) (**Figure S4**). Afternoon and pre-sleep evening activity (TLA 4pm to 12am) appeared
381 to be more heritable than morning activity (TLA 2am to 12pm). As could be expected,
382 phenotypes with higher heritability tend to have a higher average χ^2 statistic for genetic
383 associations, and a QQ plot which deviate further from the null line (**Figure S5**). The magnitude
384 of heritability estimates was generally consistent with previous studies, which reported 10-20%
385 heritability for PA traits (Doherty et al., 2018; Klimentidis et al., 2018). We also notice that
386 heritability estimated using restricted maximum likelihood (REML) tended to be slightly higher
387 Haseman-Elston regression estimates (**Figure S4**).

388

389 We further used stratified LD-score regression for partitioning heritability by functional
390 annotations of genome(Finucane et al., 2015; Finucane et al., 2018). Consistent with TWAS
391 findings, this analysis also indicated possible role for blood and immune system in addition to
392 CNS for genetic regulation of PA (**Figure 3**). In particular, heritabilities for both TLA and LIPA
393 were enriched for DNase I hypersensitivity sites (DHS) in primary B cells from peripheral blood

394 and that for TLA 12pm-2pm were enriched for H3K27ac in spleen. We also found potential
395 enrichment in other traits, though they were not significant after FDR adjustment. For example,
396 for TLA 8am-10am, MVPA, and ASTP the heritability enrichment in active chromatin regions of
397 blood/immune tissues were all close to being statistically significant (**Figure S6**).
398
399 We further used LD score regression(Bulik-Sullivan et al., 2015a; Bulik-Sullivan et al., 2015b) to
400 explore genetic correlation between PA phenotypes and four broad groups of complex traits
401 and diseases (**Figure S7**). Genetic correlations were identified (FDR < 10%) between PA
402 phenotypes and: (1) neurological, psychiatric and cognitive traits, including Alzheimer's disease
403 (AD), attention-deficit hyperactivity disorder (ADHD), depressive symptoms, intelligence, and
404 neo-conscientiousness; (2) auto-immune diseases, with the strongest correlation for multiple
405 sclerosis and weaker correlations for Crohn's disease and primary billary cirrhosis; (3) obesity-
406 related anthropometric traits and (4) cholesterol levels. Most PA traits have negative genetic
407 correlation with obesity-related traits and triglycerides, and positive genetic correlation with
408 HDL cholesterol. The directions of genetic correlation with the other two categories of traits are
409 mixed (**Figure S7**). These results broadly supported our previous results indicating the role of
410 CNS and blood/immune related mechanisms in the genetics of PA traits.
411
412 **Discussion**
413
414 In summary, our study provided novel insights to genetic architecture of physical activity
415 through genome-wide association analysis of an extensive set of accelerometry based PA

416 phenotypes, derived in the UK biobank study, and a series of follow-up genomic analyses. We
417 identified a total of six novel loci, most of which were associated with PA phenotypes not
418 considered in previous studies (Dashti et al., 2019; Doherty et al., 2018; Jones et al., 2019;
419 Klimentidis et al., 2018). Our analysis also identified novel phenotypes associated with the
420 known loci. Further, we provided multiple independent lines of evidence that genetic
421 mechanisms for association for PA involve the blood and immune system.
422
423 Compared to the 15 loci identified by the two previous GWASs on accelerometry-based PA
424 (Doherty et al., 2018; Klimentidis et al., 2018), the novel loci we discovered have increased the
425 number of PA susceptibility loci by 33%. Most of the novel loci were connected to the
426 expression of genes, pseudogenes or long non-coding RNAs (lncRNA, **Table 2 and 3**), and
427 *C3orf62* was also supported by evidence of colocalization (**Table S3**). The novel locus indexed by
428 rs9818758 overlaps with the TWAS locus index by *C3orf62*. Though it was unclear how *C3orf62*
429 is involved in PA, two secondary genes in the locus, *ARIH2* and *DAG1* (**Table 3**), appeared to be
430 involved in the following biological processes: *ARIH2* was found to be essential for
431 embryogenesis by regulating the immune system(Lin et al., 2013); *DAG1* was found to play a
432 role in the regeneration of skeletal muscles(Cohn et al., 2002). Both processes appeared
433 relevant for PA. We argue that the two loci above, supported by multiple lines of evidence
434 including GWAS, TWAS, colocalization and gene functions, should be prioritized in follow-up
435 studies. Another two novel loci were connected to pseudogene *RN7SKP16* and *PDXDC2P* of
436 which the function is less clear and may also be worth future investigation. However, Dashti et
437 al found a transcription factor site variant rs915416 to be associated with sleep duration, which

438 is approximately 930Kb away from the transcription start site of *RN7SKP1* and might have
439 potential long range regulatory effects which warrants further study. Among the genes located
440 in known loci, *PBX3* and *RP11-396F22.1* were highlighted by both TWAS and colocalization
441 results. *PBX3* is a member of the pre-B cell leukemia (PBX) family which have extensive roles in
442 early development and some adult processes (Morgan & Pandha, 2020), which could also
443 modulate its association with PA.
444
445 The novel phenotypes in this study provided important insights into the genetic architecture of
446 PA, which may have been overlooked by previous GWASs on a small number of phenotypes.
447 The accelerometry-based study by Doherty et al identified the genetic associations with overall
448 activity, sleep duration and sedentary time(Doherty et al., 2018); the study by Klimentidis et al
449 studied the average acceleration and the duration of active states(Klimentidis et al., 2018). Our
450 results found that there can be different genetic architecture for PA during different times of
451 the day, and there can be unique variants that only affect certain PA patterns, like ASTP, LIPA
452 and relative amplitude, but not others (**Table 2**). The heritability and genetic correlation can
453 also vary across different PA phenotypes (**Figures S4 and S7**).
454
455 TWAS and tissue-specific heritability enrichment analysis suggested that in addition to the CNS,
456 the blood and immune system could be also associated with PA. This finding was further
457 supported by colocalization, gene-set enrichment and genetic correlation analyses. A previous
458 study(Doherty et al., 2018), which explored enrichment of heritability for PA traits by tissue-
459 specific gene expression patterns, identified potential modulating role of the CNS,

460 adrenal/pancreatic and skeletal muscle tissues. Our study, which used a more extended set of
461 phenotypes and chromatin-state-based annotations, confirmed previous findings and further
462 highlighted the role of the blood and immune system. Though there is lack of studies on the
463 effect of immune functions on PA, previous medical literature has established the effect of PA
464 on immune functions. A study showed that higher PA is associated with elevation of T-
465 regulatory cells and lower risk for autoimmune diseases(Sharif et al., 2018). Multiple studies
466 showed that regular moderately intense PA boost immune functions in older adults and
467 protects against age-related inflammatory disorders(Dhalwani et al., 2016; Duggal, Niemiro,
468 Harridge, Simpson, & Lord, 2019; Vancampfort et al., 2017).Though the direction of causal
469 effect may not be the same as that suggested by genetic analyses, these studies supported
470 broad connections between PA and immune functions. Future studies are needed to better
471 understand the underlying mechanisms and causal directions.
472
473 In addition to the blood and immune system, TWAS and enrichment analysis also suggested
474 that the digestive system and endocrine system could be involved in modulating the genetic
475 effects on PA. The literature has also established broad connections between PA and digestive
476 and endocrine tissues. A previous study found that PA has complex effects on gastroinstestinal
477 health(Peters, De Vries, Vanberge-Henegouwen, & Akkermans, 2001): acute strenuous activity
478 may provoke gastrointestinal symptoms while low-intensity activity could have benefits.
479 Interestingly, three TWAS loci that were significant in digestive tissues were associated with PA
480 phenotypes that are proxies for meal-time activity: *PDXDC2P* with TLA 6am-8am, *RERE* with TLA
481 6pm-8PM and *KANSL1* with TLA 4pm-6pm (**Table 3**). It was also known that multiple organs in

482 the endocrine system produce hormones that regulate physiological functions of the body,
483 which can have complex bidirectional relationships with PA(Ciloglu et al., 2005; Hawkins et al.,
484 2008; Ennour-Idrissi, Maunsell, & Diorio, 2015; Alessa et al., 2017; Hackney & Saeidi, 2019).
485 Among the endocrine tissues, thyroid appeared to be modulating the genetic effect of the
486 largest number of loci. Previous studies showed that TWAS lead genes *PBX3*, *Corf62* and
487 *KANSL1* were highly expressed in thyroid (GTEx et al., 2017), and SNPs near *KANSL1* were found
488 to be associated with thyroid-stimulating hormone levels (Teumer et al., 2018). Our TWAS
489 analysis indicated that the genes associated with PA via the blood and immune system tended
490 to also be associated with the digestive and endocrine systems, but do not usually overlap with
491 the genes associated with the CNS. This suggests that the blood and immune, digestive and
492 endocrine systems may be involved in the same broad pathway that affects PA, which is
493 different from that of CNS.
494
495 It is noteworthy that the accelerometry-derived PA phenotypes in this study are not limited to
496 exercise, but include a variety of broad-sense activity patterns. In fact, we do find that several
497 phenotypes have strong genetic correlation with sleep, chronotype and other behavioral traits
498 (**Figure S7**). Therefore, when defining novel loci, we have further excluded those variants
499 previously reported to be associated with PA, sleep and circadian rhythm. However, due to the
500 nature of accelerometry, which captures the acceleration of human body, those phenotypes
501 are still essentially and broadly PA phenotypes, though they can indirectly reflect and be related
502 to other traits. Hence we still address all of them by PA phenotypes throughout the paper.
503

504 This study has a number of limitations. Though we derived a more extensive set of PA
505 phenotypes than previous studies, information was still lost when collapsing a 7-day continuous
506 times series of wrist accelerometry into 31 PA phenotypes. The ideal approach would be to
507 conduct a GWAS utilizing all the information across the 7 days of accelerometry measurements.
508 Results could outline genetic regulation of a continuous course of PA over time. The current
509 analysis of TLA during 12 non-overlapping two-hour time intervals during the day, indicated
510 that different genetic variants may affect PA during different times of the day (**Tables 2 and 3**).
511 Another limitation is that some of the phenotypes are not directly interpretable. For example,
512 the PCs of log acceleration are less interpretable than other phenotypes, such as TLA and ASTP.
513 However, they do reflect important features of physical activity and warrant further
514 investigations. A potential solution is to obtain proxy measurements that are interpretable and
515 highly correlated with PC scores.
516
517 In conclusion, we conducted association studies on a wide range of PA phenotypes and
518 identified 5 novel loci associated with PA. We found that in addition to the CNS, the blood and
519 immune system may also play an important role in the genetic mechanisms of PA, and the
520 digestive and endocrine systems could also be involved in the blood and immune pathway.
521
522 **Data Availability**
523 Data supporting the findings of this paper are available upon application to the UK Biobank
524 study. The summary statistics are publicly available via the GWAS Catalog
525 (https://www.ebi.ac.uk/gwas/) under accession numbers GCST90061408-GCST90061434.

526

527 **Supplemental Data**

528 Supplemental Data include seven figures and four tables.

529

530 **Declaration of Interests**

531 Dr. Ciprian Crainiceanu is consulting with Bayer and Johnson and Johnson on methods
532 development for wearable devices in clinical trials. The details of the contracts are disclosed
533 through the Johns Hopkins University eDisclose system and have no direct or apparent
534 relationship with the current paper. The other authors declare no conflict of interest.

535

536 **Acknowledgements**

537 The UK Biobank data was accessed via application ID 17712. Research of Drs. Guanghao Qi,
538 Diptavo Dutta and Nilanjan Chatterjee was supported by an R01 grant from the National
539 Human Genome Research Institute [1 R01 HG010480-01].

540

541 **Web Resources**

542

543 UK Biobank: https://www.ukbiobank.ac.uk/

544 fastGWA software: https://cnsgenomics.com/software/gcta/#fastGWA

545 FUSION TWAS software: http://gusevlab.org/projects/fusion/

546 COLOC R package: https://cran.r-project.org/web/packages/coloc/index.html

547 LD score regression software: https://github.com/bulik/ldsc

548 LD Hub: http://ldsc.broadinstitute.org/ldhub/

549 FUMA GWAS: https://fuma.ctglab.nl/

550 PLINK: https://www.cog-genomics.org/plink/2.0/

551 Molecular Signatures Database: http://www.broadinstitute.org/msigdb

552 Open Targets Genetics: https://genetics.opentargets.org/

553

554 **References**

555

556 Alessa, H. B., Chomistek, A. K., Hankinson, S. E., Barnett, J. B., Rood, J., Matthews, C.

557 E., . . . Tobias, D. K. (2017). Objective Measures of Physical Activity and Cardiometabolic

558 and Endocrine Biomarkers. *Med Sci Sports Exerc*, *49*(9), 1817-1825.

559 doi:10.1249/MSS.0000000000001287

560 Bulik-Sullivan, B., Finucane, H. K., Anttila, V., Gusev, A., Day, F. R., Loh, P. R., . . . Neale, B. M.

561 (2015a). An atlas of genetic correlations across human diseases and traits. *Nature*

562 *Genetics*, *47*(11), 1236-1241. doi:10.1038/ng.3406

563 Bulik-Sullivan, B. K., Loh, P. R., Finucane, H. K., Ripke, S., Yang, J., Schizophrenia Working Group

564 of the Psychiatric Genomics Consortium, . . . Neale, B. M. (2015b). LD Score regression

565 distinguishes confounding from polygenicity in genome-wide association studies. *Nature*

566 *Genetics*, *47*(3), 291-295. doi:10.1038/ng.3211

567 Buniello, A., MacArthur, J. A. L., Cerezo, M., Harris, L. W., Hayhurst, J., Malangone,

568 C., . . . Parkinson, H. (2019). The NHGRI-EBI GWAS Catalog of published genome-wide

association studies, targeted arrays and summary statistics 2019. *Nucleic Acids Research*, *47*(D1), D1005-D1012. doi:10.1093/nar/gky1120

Bycroft, C., Freeman, C., Petkova, D., Band, G., Elliott, L. T., Sharp, K., . . . Marchini, J. (2018). The UK Biobank resource with deep phenotyping and genomic data. *Nature*, *562*(7726), 203-209. doi:10.1038/s41586-018-0579-z

Ciloglu, F., Peker, I., Pehlivan, A., Karacabey, K., Ilhan, N., Saygin, O., & Ozmerdivenli, R. (2005). Exercise intensity and its effects on thyroid hormones. *Neuro Endocrinol Lett*, *26*(6), 830-834. Retrieved from https://www.ncbi.nlm.nih.gov/pubmed/16380698

Cohn, R. D., Henry, M. D., Michele, D. E., Barresi, R., Saito, F., Moore, S. A., . . . Campbell, K. P. (2002). Disruption of DAG1 in differentiated skeletal muscle reveals a role for dystroglycan in muscle regeneration. *Cell*, *110*(5), 639-648. doi:10.1016/s0092-8674(02)00907-8

Dashti, H. S., Jones, S. E., Wood, A. R., Lane, J. M., van Hees, V. T., Wang, H., . . . Saxena, R. (2019). Genome-wide association study identifies genetic loci for self-reported habitual sleep duration supported by accelerometer-derived estimates. *Nature Communications*, *10*(1), 1100. doi:10.1038/s41467-019-08917-4

De Moor, M. H., Liu, Y. J., Boomsma, D. I., Li, J., Hamilton, J. J., Hottenga, J. J., . . . Deng, H. W. (2009). Genome-wide association study of exercise behavior in Dutch and American adults. *Med Sci Sports Exerc*, *41*(10), 1887-1895. doi:10.1249/MSS.0b013e3181a2f646

Dhalwani, N. N., O'Donovan, G., Zaccardi, F., Hamer, M., Yates, T., Davies, M., & Khunti, K. (2016). Long terms trends of multimorbidity and association with physical activity in older English population. *Int J Behav Nutr Phys Act*, *13*, 8. doi:10.1186/s12966-016-0330-9

590 Doherty, A., Jackson, D., Hammerla, N., Plötz, T., Olivier, P., Granat, M. H., . . . Wareham, N. J.
591 (2017). Large Scale Population Assessment of Physical Activity Using Wrist Worn
592 Accelerometers: The UK Biobank Study. *PLoS One*, *12*(2), e0169649.
593 doi:10.1371/journal.pone.0169649
594 Doherty, A., Smith-Byrne, K., Ferreira, T., Holmes, M. V., Holmes, C., Pulit, S. L., & Lindgren, C.
595 M. (2018). GWAS identifies 14 loci for device-measured physical activity and sleep
596 duration. *Nature Communications*, *9*(1), 5257. doi:10.1038/s41467-018-07743-4
597 Duggal, N. A., Niemiro, G., Harridge, S. D. R., Simpson, R. J., & Lord, J. M. (2019). Can physical
598 activity ameliorate immunosenescence and thereby reduce age-related multi-morbidity.
599 *Nat Rev Immunol*, *19*(9), 563-572. doi:10.1038/s41577-019-0177-9
600 ENCODE Project Consortium (2012). An integrated encyclopedia of DNA elements in the human
601 genome. *Nature*, *489*(7414), 57-74. doi:10.1038/nature11247
602 Ennour-Idrissi, K., Maunsell, E., & Diorio, C. (2015). Effect of physical activity on sex hormones in
603 women: a systematic review and meta-analysis of randomized controlled trials. *Breast*
604 *Cancer Res*, *17*(1), 139. doi:10.1186/s13058-015-0647-3
605 Finucane, H. K., Bulik-Sullivan, B., Gusev, A., Trynka, G., Reshef, Y., Loh, P. R., . . . Price, A. L.
606 (2015). Partitioning heritability by functional annotation using genome-wide association
607 summary statistics. *Nature Genetics*, *47*(11), 1228-1235. doi:10.1038/ng.3404
608 Finucane, H. K., Reshef, Y. A., Anttila, V., Slowikowski, K., Gusev, A., Byrnes, A., . . . Price, A. L.
609 (2018). Heritability enrichment of specifically expressed genes identifies disease-relevant
610 tissues and cell types. *Nature Genetics*, *50*(4), 621-629. doi:10.1038/s41588-018-0081-4

611 Gamazon, E. R., Wheeler, H. E., Shah, K. P., Mozaffari, S. V., Aquino-Michaels, K., Carroll, R.
612 J., . . . Im, H. K. (2015). A gene-based association method for mapping traits using
613 reference transcriptome data. *Nature Genetics*, *47*(9), 1091-1098. doi:10.1038/ng.3367
614 Giambartolomei, C., Vukcevic, D., Schadt, E. E., Franke, L., Hingorani, A. D., Wallace, C., &
615 Plagnol, V. (2014). Bayesian test for colocalisation between pairs of genetic association
616 studies using summary statistics. *PLoS Genetics*, *10*(5), e1004383.
617 doi:10.1371/journal.pgen.1004383
618 GTEx Consortium (2017). Genetic effects on gene expression across human tissues. *Nature*,
619 *550*(7675), 204-213. doi:10.1038/nature24277
620 Gusev, A., Ko, A., Shi, H., Bhatia, G., Chung, W., Penninx, B. W., . . . Pasaniuc, B. (2016).
621 Integrative approaches for large-scale transcriptome-wide association studies. *Nature*
622 *Genetics*, *48*(3), 245-252. doi:10.1038/ng.3506
623 Hackney, A. C., & Saeidi, A. (2019). The thyroid axis, prolactin, and exercise in humans. *Curr*
624 *Opin Endocr Metab Res*, *9*, 45-50. doi:10.1016/j.coemr.2019.06.012
625 Hara, M., Hachiya, T., Sutoh, Y., Matsuo, K., Nishida, Y., Shimanoe, C., . . . Wakai, K. (2018).
626 Genomewide Association Study of Leisure-Time Exercise Behavior in Japanese Adults.
627 *Med Sci Sports Exerc*, *50*(12), 2433-2441. doi:10.1249/MSS.0000000000001712
628 Hawkins, V. N., Foster-Schubert, K., Chubak, J., Sorensen, B., Ulrich, C. M., Stancyzk, F.
629 Z., . . . McTiernan, A. (2008). Effect of exercise on serum sex hormones in men: a 12-
630 month randomized clinical trial. *Med Sci Sports Exerc*, *40*(2), 223-233.
631 doi:10.1249/mss.0b013e31815bbba9

632 Jiang, L., Zheng, Z., Qi, T., Kemper, K. E., Wray, N. R., Visscher, P. M., & Yang, J. (2019). A
633 resource-efficient tool for mixed model association analysis of large-scale data. *Nature*
634 *Genetics*, *51*(12), 1749-1755. doi:10.1038/s41588-019-0530-8
635 Jones, S. E., Lane, J. M., Wood, A. R., van Hees, V. T., Tyrrell, J., Beaumont, R. N., . . . Weedon,
636 M. N. (2019). Genome-wide association analyses of chronotype in 697,828 individuals
637 provides insights into circadian rhythms. *Nature Communications*, *10*(1), 343.
638 doi:10.1038/s41467-018-08259-7
639 Kim, J., Min, H., Oh, S., Kim, Y., Lee, A. H., & Park, T. (2014). Joint identification of genetic
640 variants for physical activity in Korean population. *Int J Mol Sci*, *15*(7), 12407-12421.
641 doi:10.3390/ijms150712407
642 Klimentidis, Y. C., Raichlen, D. A., Bea, J., Garcia, D. O., Wineinger, N. E., Mandarino, L.
643 J., . . . Going, S. B. (2018). Genome-wide association study of habitual physical activity in
644 over 377,000 UK Biobank participants identifies multiple variants including CADM2 and
645 APOE. *Int J Obes (Lond)*, *42*(6), 1161-1176. doi:10.1038/s41366-018-0120-3
646 Kyu, H. H., Bachman, V. F., Alexander, L. T., Mumford, J. E., Afshin, A., Estep, K., . . . Forouzanfar,
647 M. H. (2016). Physical activity and risk of breast cancer, colon cancer, diabetes, ischemic
648 heart disease, and ischemic stroke events: systematic review and dose-response meta-
649 analysis for the Global Burden of Disease Study 2013. *BMJ*, *354*, i3857.
650 doi:10.1136/bmj.i3857
651 Leroux, A., Di, J., Smirnova, E., Mcguffey, E. J., Cao, Q., Bayatmokhtari, E., . . . Crainiceanu, C.
652 (2019). Organizing and analyzing the activity data in NHANES. *Stat Biosci*, *11*(2), 262-287.
653 doi:10.1007/s12561-018-09229-9

Leroux, A., Xu, S., Kundu, P., Muschelli, J., Smirnova, E., Chatterjee, N., & Crainiceanu, C. (2020). Quantifying the Predictive Performance of Objectively Measured Physical Activity on Mortality in the UK Biobank. *J Gerontol A Biol Sci Med Sci*. doi:10.1093/gerona/glaa250

Liberzon, A., Subramanian, A., Pinchback, R., Thorvaldsdóttir, H., Tamayo, P., & Mesirov, J. P. (2011). Molecular signatures database (MSigDB) 3.0. *Bioinformatics*, *27*(12), 1739-1740. doi:10.1093/bioinformatics/btr260

Lightfoot, J. T., DE Geus, E. J. C., Booth, F. W., Bray, M. S., DEN Hoed, M., Kaprio, J., . . . Bouchard, C. (2018). Biological/Genetic Regulation of Physical Activity Level: Consensus from GenBioPAC. *Med Sci Sports Exerc*, *50*(4), 863-873. doi:10.1249/MSS.0000000000001499

Lin, A. E., Ebert, G., Ow, Y., Preston, S. P., Toe, J. G., Cooney, J. P., . . . Pellegrini, M. (2013). ARIH2 is essential for embryogenesis, and its hematopoietic deficiency causes lethal activation of the immune system. *Nature Immunology*, *14*(1), 27-33. doi:10.1038/ni.2478

Loh, P. R., Kichaev, G., Gazal, S., Schoech, A. P., & Price, A. L. (2018). Mixed-model association for biobank-scale datasets. *Nature Genetics*, *50*(7), 906-908. doi:10.1038/s41588-018-0144-6

Loh, P. R., Tucker, G., Bulik-Sullivan, B. K., Vilhjálmsson, B. J., Finucane, H. K., Salem, R. M., . . . Price, A. L. (2015). Efficient Bayesian mixed-model analysis increases association power in large cohorts. *Nature Genetics*, *47*(3), 284-290. doi:10.1038/ng.3190

McGregor, D. E., Palarea-Albaladejo, J., Dall, P. M., Stamatakis, E., & Chastin, S. F. M. (2019). Differences in physical activity time-use composition associated with cardiometabolic risks. *Prev Med Rep*, *13*, 23-29. doi:10.1016/j.pmedr.2018.11.006

Moore-Harrison, T., & Lightfoot, J. T. (2010). Driven to be inactive? The genetics of physical activity. *Prog Mol Biol Transl Sci*, *94*, 271-290. doi:10.1016/B978-0-12-375003-7.00010-8

Morgan, R., & Pandha, H. S. (2020). PBX3 in Cancer. *Cancers (Basel)*, *12*(2). doi:10.3390/cancers12020431

Peters, H. P., De Vries, W. R., Vanberge-Henegouwen, G. P., & Akkermans, L. M. (2001). Potential benefits and hazards of physical activity and exercise on the gastrointestinal tract. *Gut*, *48*(3), 435-439. doi:10.1136/gut.48.3.435

Piercy, K. L., Troiano, R. P., Ballard, R. M., Carlson, S. A., Fulton, J. E., Galuska, D. A., . . . Olson, R. D. (2018). The Physical Activity Guidelines for Americans. *JAMA*, *320*(19), 2020-2028. doi:10.1001/jama.2018.14854

Roadmap, E. C., Kundaje, A., Meuleman, W., Ernst, J., Bilenky, M., Yen, A., . . . Kellis, M. (2015). Integrative analysis of 111 reference human epigenomes. *Nature*, *518*(7539), 317-330. doi:10.1038/nature14248

Rock, P., Goodwin, G., Harmer, C., & Wulff, K. (2014a). Daily rest-activity patterns in the bipolar phenotype: A controlled actigraphy study. *Chronobiol Int*, *31*(2), 290-296. doi:10.3109/07420528.2013.843542

Rock, P., Goodwin, G., Harmer, C., & Wulff, K. (2014b). Daily rest-activity patterns in the bipolar phenotype: A controlled actigraphy study. *Chronobiol Int*, *31*(2), 290-296. doi:10.3109/07420528.2013.843542

Rovio, S., Kåreholt, I., Helkala, E. L., Viitanen, M., Winblad, B., Tuomilehto, J., . . . Kivipelto, M. (2005). Leisure-time physical activity at midlife and the risk of dementia and Alzheimer's disease. *Lancet Neurol*, *4*(11), 705-711. doi:10.1016/S1474-4422(05)70198-8

Schrack, J. A., Kuo, P. L., Wanigatunga, A. A., Di, J., Simonsick, E. M., Spira, A. P., . . . Zipunnikov, V. (2019). Active-to-Sedentary Behavior Transitions, Fatigability, and Physical Functioning in Older Adults. *J Gerontol A Biol Sci Med Sci*, *74*(4), 560-567. doi:10.1093/gerona/gly243

Sharif, K., Watad, A., Bragazzi, N. L., Lichtbroun, M., Amital, H., & Shoenfeld, Y. (2018). Physical activity and autoimmune diseases: Get moving and manage the disease. *Autoimmun Rev*, *17*(1), 53-72. doi:10.1016/j.autrev.2017.11.010

Smirnova, E., Leroux, A., Cao, Q., Tabacu, L., Zipunnikov, V., Crainiceanu, C., & Urbanek, J. (2019). The predictive performance of objective measures of physical activity derived from accelerometry data for 5-year all-cause mortality in older adults: NHANES 2003-2006. *J Gerontol A Biol Sci Med Sci*. doi:10.1093/gerona/glz193

Teumer, A., Chaker, L., Groeneweg, S., Li, Y., Di Munno, C., Barbieri, C., . . . Medici, M. (2018). Genome-wide analyses identify a role for SLC17A4 and AADAT in thyroid hormone regulation. *Nature Communications*, *9*(1), 4455. doi:10.1038/s41467-018-06356-1

Vancampfort, D., Koyanagi, A., Ward, P. B., Rosenbaum, S., Schuch, F. B., Mugisha, J., . . . Stubbs, B. (2017). Chronic physical conditions, multimorbidity and physical activity across 46 low- and middle-income countries. *Int J Behav Nutr Phys Act*, *14*(1), 6. doi:10.1186/s12966-017-0463-5

Watanabe, K., Taskesen, E., van Bochoven, A., & Posthuma, D. (2017). Functional mapping and annotation of genetic associations with FUMA. *Nature Communications*, *8*(1), 1826. doi:10.1038/s41467-017-01261-5

718 Watanabe, K., Umićević Mirkov, M., de Leeuw, C. A., van den Heuvel, M. P., & Posthuma, D.
719 (2019). Genetic mapping of cell type specificity for complex traits. *Nature*
720 *Communications*, *10*(1), 3222. doi:10.1038/s41467-019-11181-1
721 Young, D. R., & Haskell, W. L. (2018). Accumulation of Moderate-to-Vigorous Physical Activity
722 and All-Cause Mortality. *J Am Heart Assoc*, *7*(6). doi:10.1161/JAHA.118.008929
723 Zheng, J., Erzurumluoglu, A. M., Elsworth, B. L., Kemp, J. P., Howe, L., Haycock, P. C., . . . Neale,
724 B. M. (2017). LD Hub: a centralized database and web interface to perform LD score
725 regression that maximizes the potential of summary level GWAS data for SNP heritability
726 and genetic correlation analysis. *Bioinformatics*, *33*(2), 272-279.
727 doi:10.1093/bioinformatics/btw613
728
729
730

Table 1. Description of physical activity phenotypes.

Category	Phenotype abbreviation	Phenotype full name and description
Total volume of activity	TA*	Total acceleration.
	TLA	Total log acceleration. Sum of log(1+acceleration).
Activity during 2-hour windows of the day	TLA 12am-2am, TLA 2am-4am, TLA 4am-6pm, …, TLA 8pm-10pm, TLA 10pm-12am	Total log acceleration in the k-th two-hour window of the day, starting from midnight (12 intervals in total)
Duration of activity patterns	ST*	Duration of sedentary state. Time when the acceleration is less than 30 milli-gravity (mg) is defined as sedentary state.
	LIPA	Duration of light-intensity physical activity (LIPA). LIPA is defined as the time when the acceleration is >=30mg but <100mg.
	MVPA	Duration of moderate to vigorous physical activity (MVPA). MVPA is defined as the time when the acceleration if >=100mg.
Principal components	PC1*, PC2, …, PC6	First 6 principal component of the log-transformed minute-level activity profiles.
Active-sedentary transition patterns	SATP	Sedentary to active transition probability. SATP is the probability of transitioning to active state if the subject is currently sedentary. Active state is defined as acceleration >=30mg and sedentary state is defined as acceleration <30mg.
	ASTP	Active to sedentary transition probability. SATP is the probability of transitioning to sedentary state if the subject is currently active.
Circadian rhythm proxies	DARE	Dynamic activity ratio estimate. Total log-acceleration during 8am-8pm as proportion of TLA for the whole day.
	M10*	Average log acceleration during the ten most active hours of the day
	L5	Average log acceleration during the five least active hours of the day
	Timing of M10	Mid-point of the ten most active hours of the day
	Timing of L5	Mid-point of the five least active hours of the day
	Relative amplitude	Relative amplitude = (M10-L5)/(M10+L5). It measures the difference between daytime activity and activity during sleep.

All the phenotypes are first calculated at the day level and then averaged across 7 days.
***** Excluded from genetic association analyses due to high correlation (>0.8) with TLA.

Table 2. Significant loci associated with physical activity in single-variant analysis.

Lead variant[a]	Chromosome region	Base pair	Minor allele	Major allele	Minor allele frequency	Nearest coding gene and distance[d]	Significantly associated traits[c]	Previous studies that discovered the locus
Novel loci[b]								
rs3836464	3p25.3	10454772	CA	C	0.274	SEC13 (92kb)	ASTP (p=2.2e-09, b=-0.032)	NA
rs9818758	3p21.31	49382925	A	G	0.171	USP4 (4.8kb)	Relative amplitude (p=2.1e-09, b=-0.036)	
3:131647162_TA_T	3q22	131647162	T	TA	0.466	CPNE4 (357kb)	TLA 2am-4am (p=2.2e-09, b=0.029)	
Known loci								
rs1144566	1q25.3	182569626	T	C	0.030	RGS16 (3.9kb)	Timing of L5 (p=5e-10, b=-0.086)*	4
rs301799	1p36.23	8489302	C	T	0.422	SLC45A1 (111kb)	TLA 6pm-8pm (p=1.7e-09, b=0.027)*	OTG[e]
rs113851554	2p14	66750564	T	G	0.050	MEIS1 (90kb)	TLA 12am-2am (p=6.7e-37, b=0.138)*, TLA 2am-4am (p=7.9e-39, b=0.142)*, L5 (p=1.3e-33, b=0.13)*, Relative amplitude (p=6.9e-15, b=-0.082)*, Timing of L5 (p=5.4e-22, b=0.105)*	1,4
rs2909950	5q33.1	151886147	A	G	0.418	NMUR2 (73kb)	TLA 6pm-8pm (p=9.4e-10, b=-0.028)*	4
rs12717867	5q33.1	152412845	G	A	0.453	GRIA1 (456kb)	LIPA (p=6.2e-10, b=-0.029)*	4
rs9369062	6p21.2	38437303	C	A	0.292	BTBD9 (171kb)	TLA 12am-2am (p=1.5e-12, b=-0.037)*, TLA 2am-4am (p=2.3e-10, b=-0.033)*	4
rs2006810	7q11.22	69902152	C	T	0.395	GALNT17 (695kb)	TLA 8pm-10pm (p=8.1e-11, b=-0.031)*	1,4
rs1268539	9q33.3	128195657	A	C	0.419	GAPVD1 (172kb)	TLA (p=1.1e-10, b=0.03), LIPA (p=3.2e-10, b=0.03)*	1
rs564819152	10p12.31	21820650	G	A	0.320	SKIDA1 (5kb)	TLA 8am-10am (p=1.4e-09, b=-0.031)*	1,3
rs2138543	12q12	39298423	A	T	0.477	CPNE8 (2.8kb)	TLA 6am-8am (p=3.9e-11, b=0.03)*, PC2 (p=1.5e-09, b=-0.029)*	4
rs12927162	16q12.2	52684916	G	A	0.277	TOX3 (103kb)	TLA 10pm-12am (p=1e-09, b=0.032)*	4
rs2532402	17q21.31	44304130	G	C	0.221	KANSL1 (1.4kb)	TLA (p=1.5e-12, b=0.04), MVPA (p=1.9e-10, b=0.035)	1,2,3,4
rs3837946	19p13.2	9955920	TTTTG	T	0.475	PIN1 (10kb)	TLA (p=1.3e-11, b=-0.032), LIPA (p=1.6e-09, b=-0.029)*	1,3

[a]Significant variants (single nucleotide polymorphism (SNP) or insertion/deletion) are defined as those with fastGWA p-value $< 2.63 \times 10^{-9}$ (Bonferroni corrected for 19 independent traits). LD clumping was performed at $r^2 < 0.1$ and lead variants of different loci were required to be >500kb apart.
[b]A locus is defined as novel if its lead variant is >500kb from the lead variant of any loci identified in one of the previous GWAS: 1) Doherty et al study on a smaller set of accelerometry-based physical activity; 2) Klimentidis et al study on self-reported and accelerometry based physical activity; 3) Dashti et al study on self-reported sleep duration; 4) Jones et al study on circadian rhythm. Loci that were discovered by the four above studies are marked with 1, 2, 3 and 4 in the last column, respectively. Novel phenotypes associated with known loci are marked with *.
[c]Traits are followed by p-values (p) and effect sizes (b). The effects size b is for the effect of minor allele vs major allele, e.g. a positive b indicates the minor allele is the trait-increasing allele. TLA: total log-acceleration. ASTP: active-to-sedentary transition probability. MVPA: moderate-to-vigorous physical activity. PC2: second principal component. LIPA: light-intensity physical activity.
[d]Nearest coding gene is defined as the protein-coding gene whose transcription start site (TSS) is closest to the variant.
[e]This locus was not reported by the four studies we catalogued but was associated with daytime nap, as reported by Open Targets Genetics (OTG). See Table S4 for details.

Table 3. Significant loci associated with physical activity identified in transcriptome-wide association studies (TWAS).

Most significant gene[a]	CHR	Gene start	Gene end	Locus	Minimum p-value across traits and tissues	Secondary genes in the locus with comparable associations[c]	Trait and tissue[d]	Previous studies that discovered the locus
Novel loci[b]								
RN7SKP16	1	33802167	33802465	1p35.1	2.72E-09	-	MVPA (CNS)	
PDXDC2P	16	70069541	70098679	16q22.1	1.81E-09	-	TLA 6am-8am (Blood/Immune, Digestive)	NA
Known loci								
RERE†	1	8412457	8877702	1p36.23	5.28E-09	*ENO1-IT1, RP5-1115A15.1*†	TLA 6pm-8pm (Digestive, Other, Blood/Immune)	GWAS
RP5-1160K1.6	1	110171118	110171939	1p13.3	7.68E-10	-	PC2 (CNS)	4
C3orf62†	3	49306219	49315263	3p21.31	3.28E-10	*RP11-694I15.7, ARIH2, DAG1, SLC25A20*	Relative amplitude (Digestive, Endocrine)	GWAS
CTC-467M3.3	5	87988462	87989789	5q14.3	1.39E-08	-	ASTP (CNS)	1,4
NMUR2	5	151771093	151812929	5q33.1	8.88E-10	-	TLA 6pm-8pm (CNS, Other)	4,GWAS
PBX3†	9	128509624	128729656	9q33.3	3.04E-10	*MAPKAP1*	LIPA (Blood/Immune, Digestive, Endocrine, Other); SATP (Blood/Immune, Other, Digestive, Endocrine); TLA (Blood/Immune, Other, Digestive, Endocrine)	1,GWAS
DNAJC1	10	22045466	22292698	10p12.31	3.20E-09	*CASC10*†	TLA 8am-10am (CNS)	1,3,GWAS
RP11-396F22.1†	12	39300253	39303394	12q12	9.89E-10	-	Timing of M10 (CNS), PC2 (CNS, Other), TLA 6am-8am (CNS, Other)	4,GWAS
FMNL1	17	43299590	43324633	17q21.31	2.82E-09	*CTD-2020K17.1*	TLA (CNS)	1,4
KANSL1	17	44107282	44302733	17q21.31	2.17E-13	*KANSL1-AS1, RP11-798G7.8*	MVPA (CNS, Blood/Immune, Other, Digestive, Musculoskeletal/connective); TLA 4pm-6pm (Blood/Immune, Other, Digestive); TLA (Adipose, CNS, Blood/Immune, Other, Digestive, Cardiovascular, Musculoskeletal/connective, Endocrine)	1,2,3,4,GWAS
ZNF846	19	9862669	9903856	19p13.2	2.22E-10	*OLFM2, PIN1, CTD-2623N2.3*	TLA (Other)	1,3,GWAS
JUND	19	18390563	18392432	19p13.11	3.18E-09	-	SATP (Other)	4
LINC00634	22	42348169	42354937	22q13.2	4.85E-11	-	TLA (CNS)	4

[a]For each gene, we apply Benjamini-Hochberg (BH) correction across all trait-tissue pairs. Significant genes are defined as those with BH corrected p-value $< 2.5 \times 10^{-6}$. Significant genes are clustered using an approach similar to LD clumping so that different loci, marked by the transcription start site (TSS) of the lead gene, are >1Mb apart. Gene symbols are italicized. † Genes of which the eQTL signal colocalizes with GWAS signal of the most significantly associated phenotype.

[b]A locus is defined as novel if its flanking region ($\pm$500kb from TSS) does not harbor a variant reported in Table 2 or any of the four previous studies considered in Table 2. Loci that were discovered by the above studies are marked with 1, 2, 3 and 4 in the last column, respectively. Loci that were discovered by our single-variant analysis (Table 2) are marked with "GWAS" in the first column.

[c]Other genes in the cluster with minimum p-value less that 10 times the minimum p-value of the lead gene are shown in column "Secondary genes in the locus with comparable associations". See Table S2 for all the significant tissue-trait pairs.

[d]CNS: central nervous system. TLA: total log-acceleration. ASTP: active-to-sedentary transition probability. SATP: sedentary-to-active transition probability. MVPA: moderate-to-vigorous physical activity. PC2: second principal component.

Figures

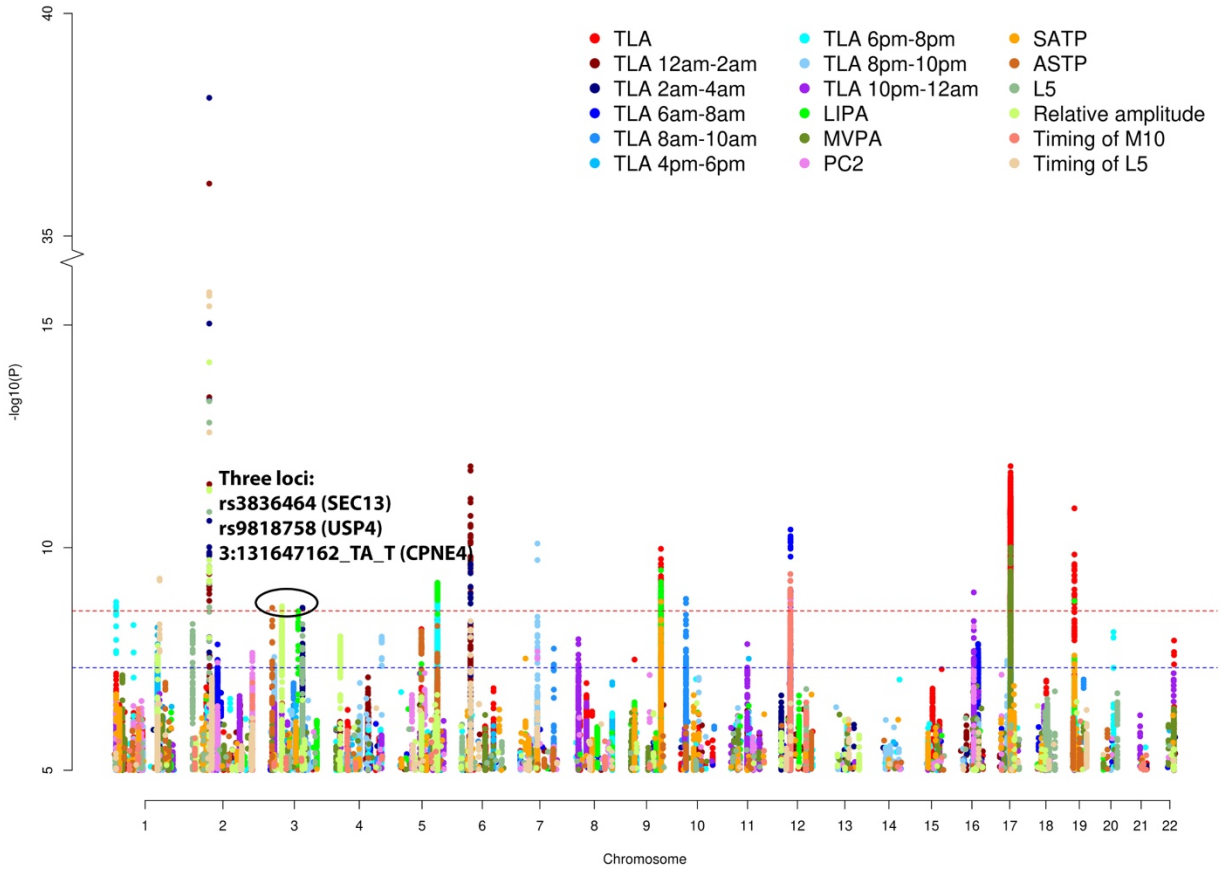

Figure 1. Manhattan plot for 18 traits that are significantly associated with at least one variant at $p < 2.63 \times 10^{-9}$ in single-variant analysis. The red dashed line is $p = 2.63 \times 10^{-9}$ accounting for the number of independent traits. The blue dashed line is the standard genome-wide significance threshold $p = 5 \times 10^{-8}$. Three novel loci that have not been discovered in previous GWAS of physical activity, sleep duration and circadian rhythm are circled out and annotated by the lead variant and nearest coding gene (see Table 2).

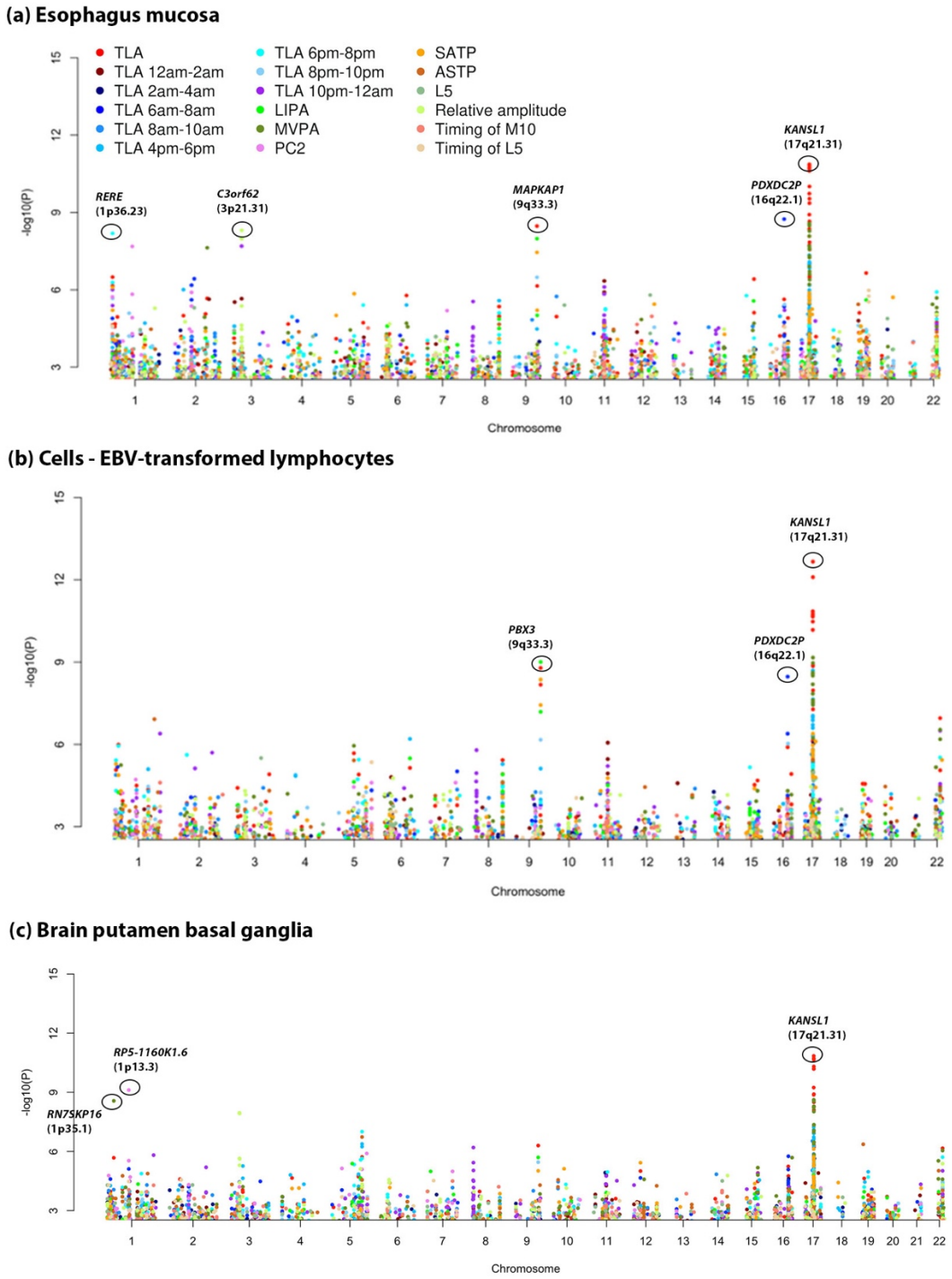

Figure 2: TWAS Manhattan plots for three tissues that harbor the TWAS novel loci. Significant genes with FDR corrected p-values$< 2.5 \times 10^{-6}$ are circled (see Methods for details). Only the PA traits that are significantly associated with at least one variant at $p < 2.63 \times 10^{-9}$ in single-variant analysis are shown.

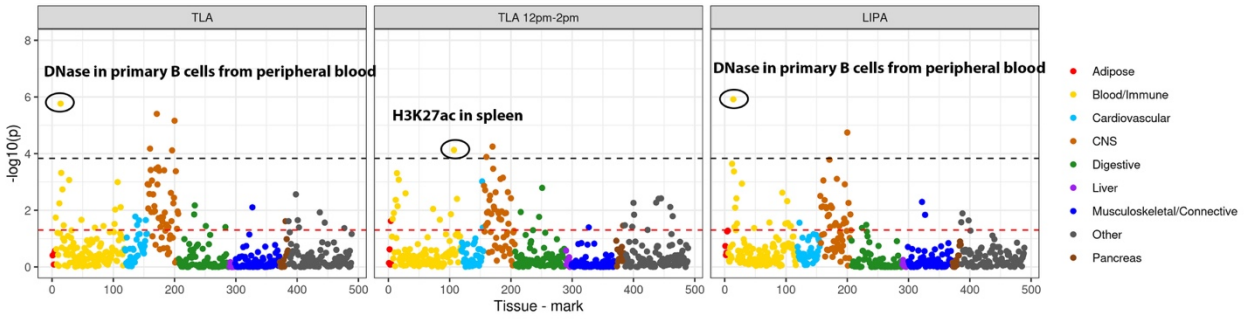

Figure 3. Tissue-specific heritability enrichment p-values for traits with significant enrichment at FDR < 0.05 in blood and immune tissues. The analysis was conducted using tissue/cell type specific stratified LD score regression based on 6 chromatin-based annotations in 111 tissues and cell types described in Finucane et al, Nature Genetics 2018 (PMID: 29632380). Each dot corresponds to an annotation in a tissue or cell type. A complete list of tissue and cell types is provided in Supplementary Table 7 of the above paper. Black line corresponds to FDR < 0.05 (-log(p-value)=3.83) across all combinations of trait, tissue, and histone mark. Red line corresponds to p = 0.05. See Figure S6 for the enrichment p-values for the rest of the traits. CNS: central nervous system.